J. Fluid Mech. (1976), *vol.* 76, *part* 4, *pp.* 625–640

Printed in Great Britain

The shape of free jets of water under gravity

By E. O. TUCK

Applied Mathematics Department, University of Adelaide, South Australia 5001

(Received 5 August 1975)

A study is made of the form taken by a slender jet of water whose only boundary is a free surface. The only forces acting are inertial and gravitational. Attention is paid to the cross-flow velocity components and to the development of the shape of the cross-section of the jet as it progresses. It is established that a jet with initially elliptic cross-sections can remain elliptical, and the variation in the aspect ratio along the jet is determined.

1. Introduction

A jet of water emerging from an upward-inclined nozzle travels in a more or less parabolic arc. Elementary momentum arguments can be used to establish that the behaviour of the jet is equivalent to that of a free ballistic projectile with the same initial velocity vector, providing the jet is sufficiently thin. Thus the velocity vector is directed along the jet, and is a combination of a uniform horizontal velocity and a vertical velocity varying like the square root of distance below the top of the arc.

The above is essentially a 'zero-order' result in the thickness of the jet. In fact the velocity vector must contain in addition cross-flow components of the order of the thickness. This is demanded by mass conservation, owing to the variation along the jet of the main velocity component. These cross-flow velocities then influence the shape of the ballistic trajectory and determine the shape of the cross-section of the jet. The zero-order result tells us nothing about the shape of the cross-sections, so long as their length scale is small compared with the length scale for changes along the jet.

The last restriction is the natural requirement for a 'one-dimensional flow', as in hydraulics (e.g. Streeter 1961, ch. 3) or gasdynamics in pipes (e.g. Shapiro 1953, ch. 8). In such one-dimensional situations with known pipe boundaries, attention is normally concentrated on the main flow as an unknown. Here (and see also Tuck 1974) the situation is somewhat different in that the main flow is relatively well known, but the 'pipe' boundary is to be determined. The additional condition which enables such a determination to be made is the constant-pressure free-surface condition.

In the case of purely two-dimensional flow, Keller & Wietz (1957) have provided an analysis of thin free sheets of water, equivalent in a number of respects to that in the present paper. They adapt the distortion procedure used by Friedrichs (1948) for deriving the shallow-water theory of water waves, in which

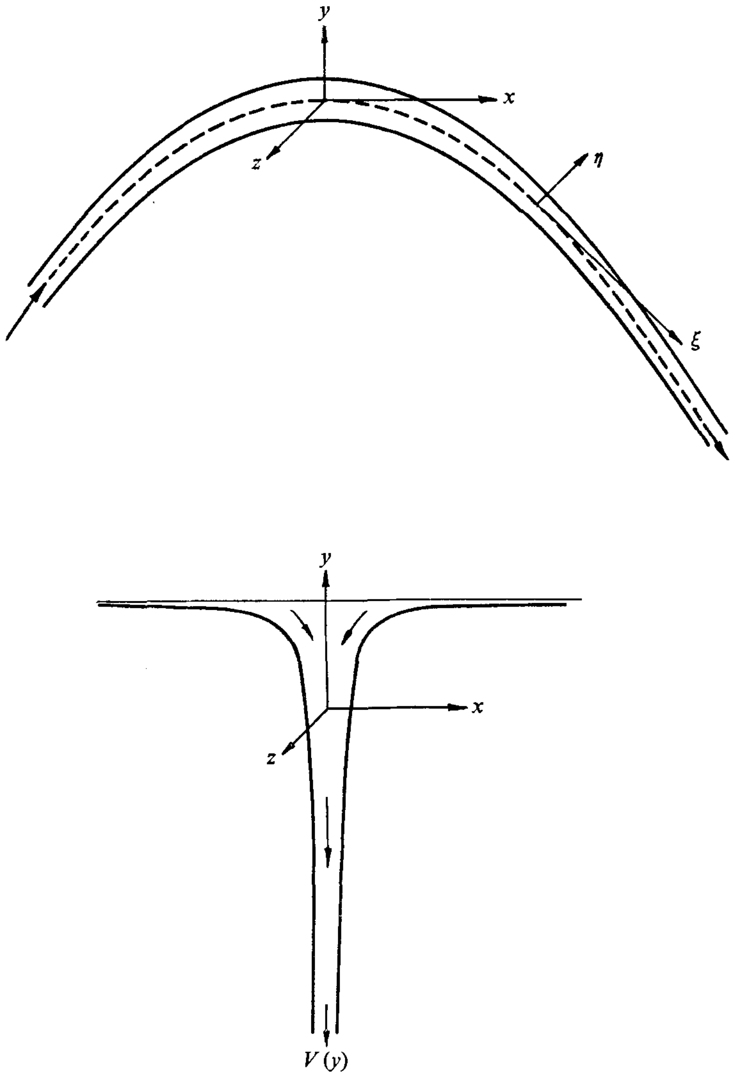

FIGURE 1. Sketch of shape of vertical and non-vertical free jets, and indication of co-ordinates.

the vertical length scale is assumed much smaller than the horizontal scale, and obtain an asymptotic expansion in terms of the ratio of these length scales. More recently, Keller & Geer (1973) have used for two-dimensional flow an inverted asymptotic expansion (space co-ordinates as functions of complex potential) which also has the property of being valid for vertical jets.

The two types of flow considered in the present paper are illustrated in figure 1. If the main flow has a non-zero horizontal velocity component we obtain the true parabolic arc discussed above. However, there is also considerable interest in the somewhat simpler problem where the horizontal velocity vanishes, and the jet is wholly rising or wholly falling. In either case the velocity increases indefinitely (and therefore the jet becomes ever thinner) as the co-ordinate y

tends to minus infinity, just as would the velocity of a projectile allowed to fall for ever. The vertical jet has the additional bizarre feature that it must spread out to an infinite radius at the y value where its main velocity vanishes. This must eventually cause the one-dimensional assumption to fail, but one would in any case normally expect to have matched the flow to an exit flow from a rigid container at a y value below that for stagnation.

Such matching has been the aim of a number of authors recently, e.g. Keady (1973) and Conway (1967) for the vertical case, Clarke (1965) for a special case of the parabolic-arc jet where the initial velocity is horizontal, and Keller & Geer (1973) for a general class of problems. The above investigations all concern solely two-dimensional flows. No comparable analyses including gravity seem to have been published for three-dimensional jets, even in the axisymmetric vertical case.

There is however a substantial body of literature (see e.g. Chandrasekhar 1968, ch. 12; Lamb 1932, §273; Rayleigh 1945, ch. 20; Keller, Rubinow & Tu 1973) on instability of cylindrical columns of flowing liquid, in the absence of gravity but under the influence of surface tension. Axisymmetric waves of small amplitude grow owing to surface-tension effects if their wavelength along the jet exceeds the circumference. The maximum growth rate occurs at about one and a half times that wavelength, and is such as to double the size of the disturbance in 0·09 s for a 1 cm diameter jet. This instability is ultimately responsible for the disintegration of the jet, but its influence can be postponed for sufficiently thick jets of sufficiently high speed, and is reduced by gravitational and viscous effects.

Rayleigh (1945, §358) also discusses experimental observations of Bidone and others on variations in the cross-section of jets with other than circular initial sections. For example (p. 355), "...in the case of an elliptical aperture with major axis horizontal, the sections of the jet taken at increasing distances gradually lose their eccentricity until at a certain distance the section is circular. Further out the section again assumes ellipticity, but now with the major axis vertical and (in the circumstances of Bidone's experiments) the ellipticity increases until the jet is reduced to a flat sheet in the vertical plane, very broad and thin. This sheet preserves its continuity to a considerable distance (e.g. six feet) from the orifice, where finally it is penetrated by air... ." The present theory generates solutions confirming these observations, which can be repeated by anyone using a garden hose. Taylor (1960; see also Longuet-Higgins 1972) provided a treatment of this problem neglecting gravity, and the present analysis can be interpreted as an extension of Taylor's work to include gravity.

We suppose the fluid to be inviscid and incompressible, and to be moving steadily and irrotationally with velocity

$$\mathbf{q} = \nabla\phi(x, y, z), \tag{1.1}$$

where

$$\nabla^2\phi = \phi_{xx} + \phi_{yy} + \phi_{zz} = 0. \tag{1.2}$$

The only boundaries of the flow are free surfaces, on which the velocity potential satisfies a kinematic condition of zero normal velocity, i.e.

$$\mathbf{n}.\mathbf{q} = \partial\phi/\partial n = 0, \tag{1.3}$$

where $\mathbf{n}$ is a unit outward normal, and in addition a dynamic free-surface boundary condition. We neglect surface tension, and therefore must require that the pressure is equal to atmospheric pressure p_A on the boundary. Bernoulli's equation states that

$$p/\rho + \tfrac{1}{2}q^2 + gy = p_A/\rho + \tfrac{1}{2}U^2 + gy_0, \tag{1.4}$$

where y is a co-ordinate measured vertically upward, and where the velocity magnitude q takes the value U and the pressure is atmospheric at $y = y_0$.

In the following analysis we shall use a non-dimensional formulation in which U is taken as a velocity scale, and U^2/g as a length scale. Thus we set

$$\mathbf{q} = U\mathbf{q}^*, \tag{1.5}$$

$$y = y_0 + (U^2/g)\,y^*, \tag{1.6}$$

$$p = p_A + \tfrac{1}{2}\rho U^2 p^*, \tag{1.7}$$

etc., but immediately drop the stars on all normalized quantities. The Bernoulli equation (1.4) gives for p (which is now in fact a pressure *coefficient*)

$$-p = q^2 + 2y - 1, \tag{1.8}$$

and the dynamic free-surface condition is that $p = 0$ on the boundary of the jet.

The problem so normalized is characterized by a non-dimensional parameter ϵ measuring the strength or thickness of the jet. If δ denotes the dimensional volume flux in the jet, then the quantity δ/U is a measure of the dimensional cross-sectional area of the jet and $(\delta/U)^{\frac{1}{2}}$ a measure of its actual lateral dimensions. The corresponding non-dimensional thickness measure is

$$\epsilon = \frac{g}{U^2}(\delta/U)^{\frac{1}{2}} = g\delta^{\frac{1}{2}}U^{\frac{5}{2}}, \tag{1.9}$$

which we take as our fundamental small parameter. The quantity ϵ can also be interpreted as the inverse square of a Froude number. Our aim in the present paper is to construct an asymptotic expansion for small ϵ.

2. Vertical motion

Consider a rising ($V > 0$) or falling ($V < 0$) body of water, symmetrical about $x = 0$ and bounded by free surfaces $x = \pm X(y,z)$, where $X = O(\epsilon)$. We suppose that the dominant velocity in this jet is $V(y)$ in the y direction, where $V = O(1)$ with respect to the small parameter ϵ, and is to be determined. We set

$$\phi = \phi_0(y) + \Phi(x,y,z), \tag{2.1}$$

where $\phi_0'(y) = V(y)$ and where the cross-flow potential Φ is small. In fact $\Phi = O(\epsilon^2)$ in this problem, as we shall see.

The one-dimensional character of the flow in the limit as $\epsilon \to 0$ requires that all quantities vary more slowly in the main direction of flow than normal to it; specifically $\partial/\partial y = O(1)$ but $\partial/\partial x$, $\partial/\partial z = O(\epsilon^{-1})$. The exact equation for Φ, namely [from (1.2)]

$$\Phi_{xx} + \Phi_{yy} + \Phi_{zz} = -V'(y),$$

is therefore approximated with an error $O(\epsilon^2)$ by

$$\Phi_{xx} + \Phi_{zz} = -V'(y). \tag{2.2}$$

Similarly, the exact kinematic boundary condition on $x = \pm X(y,z)$, namely [from (1.3)]

$$\Phi_x \mp X_z \Phi_z = \pm (V + \Phi_y) X_y,$$

is likewise approximated by

$$\Phi_x \mp X_z \Phi_z = \pm V X_y. \tag{2.3}$$

In classical one-dimensional flows in pipes of known geometry the problem of determining the cross-flow velocities consists (see Tuck 1974) of solving the two-dimensional Poisson equation (2.2) in the interior portion $|x| < X$ of the x, z plane, subject to (2.3), which prescribes the normal velocity on the cross-section $x = X$ in that plane.

Continuity demands that the net flux given by (2.3) exactly balances the rate of production of volume by the source term on the right of (2.2). Thus

$$\iint_{|x|<X} (\Phi_{xx} + \Phi_{zz})\, dy\, dz = \oint_{(x=X)\,+\,(x=-X)} \frac{\partial \Phi}{\partial n}\, dl,$$

or

$$-V'(y)\, S(y) = 2\int V X_y\, dz = V S'(y), \tag{2.4}$$

where $S(y) = 2\int X(y,z)\, dz$ is the cross-sectional area at station y. That is, from (2.4) we have

$$V(y)\, S(y) = \text{constant}, \tag{2.5}$$

which is the ordinary one-dimensional continuity equation or Venturi law, and can be obtained by elementary means.

In the present case, the boundary equation $X(y,z)$ is unknown, and the problem formulation is completed by use of the dynamic free-surface condition (1.8). The exact expression for the pressure becomes

$$-p = (V + \Phi_y)^2 + \Phi_x^2 + \Phi_z^2 + 2y - 1,$$

which reduces to

$$-p = (V^2 + 2y - 1) + (2V\Phi_y + \Phi_x^2 + \Phi_z^2) \tag{2.6}$$

on neglect of the $O(\epsilon^4)$ term Φ_y^2. The $O(1)$ terms in (2.6) vanish if

$$V = \pm (1 - 2y)^{\frac{1}{2}}, \tag{2.7}$$

and if (2.7) is true the pressure coefficient is $O(\epsilon^2)$ throughout the jet. The dynamic boundary condition requires that the $O(\epsilon^2)$ part also vanishes on $x = \pm X$, so that

$$2V\Phi_y + \Phi_x^2 + \Phi_z^2 = 0. \tag{2.8}$$

The task confronting us then is to solve (2.2) subject to both (2.3) and (2.8) on the unknown boundary $x = \pm X(y,z)$. This task is clearly a formidable one in general, and we present here solutions only for the case of elliptic sections. Of course, an even simpler special case is the two-dimensional case of a thin vertical sheet of water, and the present method produces results for this case equivalent to those of Keller & Geer (1973) and others.

3. Vertical jets with elliptic sections

We now seek a solution of (2.2) of the form

$$\Phi = A(y) + C(y)\,x^2 + D(y)\,z^2, \tag{3.1}$$

where $A(y)$, $C(y)$ and $D(y)$ are to be determined. Equation (2.2) is satisfied if

$$C + D = -\tfrac{1}{2}V'. \tag{3.2}$$

We also assume that the sections have an elliptic form, with

$$X^2(y,z) = a^2(y) - \gamma^2(y)\,z^2, \tag{3.3}$$

where $a(z)$ is the (unknown) semi-axis in the x direction and $b(z) = a(z)/\gamma(z)$ is the semi-axis in the z direction.

On substitution of (3.1) and (3.3) in the kinematic boundary condition (2.3), we have

$$2XC + 2zD(\gamma^2 z/X) = (V/X)\,(aa' - \gamma\gamma' z^2),$$

or

$$(2Ca^2 - Vaa') + z^2(2D\gamma^2 - 2C\gamma^2 + V\gamma\gamma') = 0, \tag{3.4}$$

which is satisfied for all z on the cross-section if and only if

$$C = \tfrac{1}{2}V(a'/a), \quad \text{and} \quad C - D = \tfrac{1}{2}V(\gamma'/\gamma). \qquad (3.5),\ (3.6)$$

Equations (3.2) and (3.6) together imply

$$-4C = V' - V(\gamma'/\gamma), \quad -4D = V' + V(\gamma'/\gamma), \qquad (3.7),\ (3.8)$$

and from (3.5) and (3.7) we deduce

$$2a'/a + V'/V = \gamma'/\gamma,$$

or

$$a^2 V/\gamma = \text{constant},$$

which is a re-statement of the continuity equation (2.5), since $S = \pi ab = \pi a^2/\gamma$.

Turning to the dynamic free-surface condition (2.8), we have on $x = X$

$$2V(A' + C'x^2 + D'z^2) + 4C^2x^2 + 4D^2z^2 = 0,$$

i.e.

$$(2VA' + 2VC'a^2 + 4C^2a^2) + z^2(-2VC'\gamma^2 + 2VD' - 4C^2\gamma^2 + 4D^2) = 0, \tag{3.9}$$

which is true for all z if

$$A' = -a^2(C' + 2C^2/V) \tag{3.10}$$

and

$$VD' + 2D^2 = \gamma^2(VC' + 2C^2). \tag{3.11}$$

Equation (3.10) ultimately determines the quantity $A(y)$ and will not concern us further in the present paper. Note that neither $A(y)$ nor $a(y)$ appears in (3.11), which now becomes an equation to determine the aspect ratio $\gamma(y)$ of the ellipse. On elimination of $C(y)$ by use of (3.2), and use of (2.11) and (2.12) we have

$$VD'(1+\gamma^2) + 2D^2(1-\gamma^2) = (\gamma^2/V^2)\,(1-2DV). \tag{3.12}$$

It is convenient to use $\xi = -V(y)$ as independent variable instead of y itself, writing

$$D'(y) = \xi^{-1}\,dD/d\xi.$$

Thus
$$(1+\gamma^2)\frac{dD}{d\xi}+2(1-\gamma^2)D^2 = \frac{\gamma^2}{\xi^2}(1+2D\xi), \tag{3.13}$$

which is supplemented by (3.8), namely
$$d\gamma/d\xi = -\gamma(4D+1/\xi). \tag{3.14}$$

The quantity D can be eliminated between (3.13) and (3.14), leading to a non-linear second-order ordinary differential equation for $\gamma(\xi)$. For *falling* jets ($\xi > 0$) it is convenient to make the change of variables
$$\gamma^2 = \lambda, \quad \xi = e^t, \qquad (3.15), (3.16)$$

and we find that $\lambda = \lambda(t)$ then satisfies
$$\ddot{\lambda} = 2\dot{\lambda}+\frac{3\lambda(1-\lambda)}{1+\lambda}+\frac{5+3\lambda}{4\lambda(1+\lambda)}\dot{\lambda}^2, \tag{3.17}$$

where dots denote d/dt.

It is notable that the independent variable t does not appear explicitly in (3.17) and thus the solution trajectories can be studied in the $\lambda, \dot{\lambda}$ phase plane, by solution of the first-order equation
$$\frac{d\dot{\lambda}}{d\lambda} = 2+\frac{3\lambda(1-\lambda)}{1+\lambda}\frac{1}{\dot{\lambda}}+\frac{5+3\lambda}{4\lambda(1+\lambda)}\dot{\lambda}. \tag{3.18}$$

Another notable feature of (3.17) is that if $\lambda(t)$ satisfies (3.17) then so does $1/\lambda(t)$. This feature is expected from the lateral symmetry of the problem, and simply corresponds to an interchange of semi-axes of the ellipse.

Trajectories obtained by numerical solution of (3.18) are shown in figure 2. The critical or equilibrium points are a stable node at the origin $\lambda = \dot{\lambda} = 0$ and an unstable focus at $\lambda = 1$, $\dot{\lambda} = 0$. In the neighbourhood of $\lambda = 1$, $\dot{\lambda} = 0$, the cross-section is almost circular, but its eccentricity takes alternately positive and negative values as we proceed along the jet and the trajectory spirals out in a clockwise manner. Note however that this spiral has a very large rate of increase of radius (asymptotically a factor of $\exp(2\pi\sqrt{2}) \simeq 7000$ times per revolution), so that on the scale of figure 2 very few oscillations can be seen. The immediate neighbourhood of the point $\lambda = 1$, $\dot{\lambda} = 0$ corresponds to the start of the flow at $t = -\infty$ or $\xi = 0$, as a circular column with zero velocity and therefore infinite cross-sectional area. When the lateral length scale becomes large enough to be comparable with the length scale for changes *along* the jet, the one-dimensional assumption breaks down, and other factors need to be considered. The behaviour shown in this region is related to the Rayleigh instability discussed in the introduction.

The ultimate destination of all trajectories is either $\lambda = 0$ or $\lambda = \infty$. If the former, the trajectory asymptotes to the origin along
$$\dot{\lambda} = -6\lambda,$$

i.e. we have
$$\lambda \propto e^{-6t} = \xi^{-6},$$

or $\gamma \propto \xi^{-3}$. All trajectories which start 'below' a certain critical trajectory, whose approximate location is shown dashed in figure 2, ultimately have the

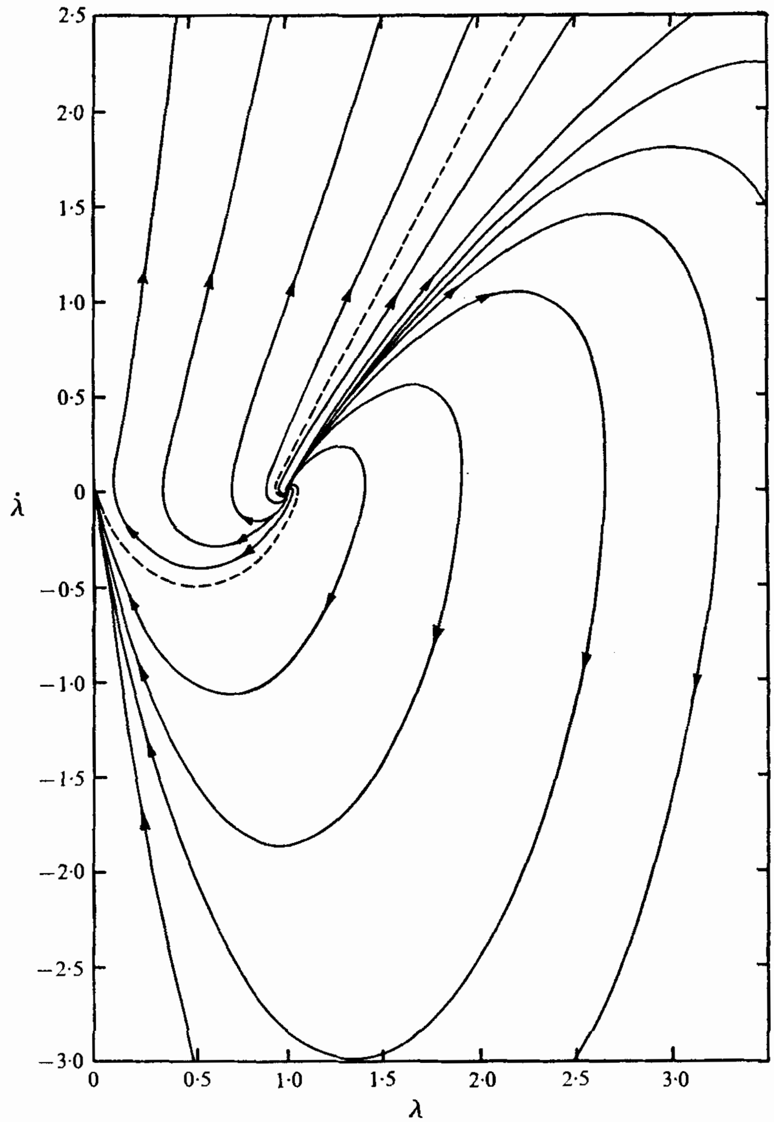

FIGURE 2. Phase-plane trajectories for $\dot{\lambda}$ against λ, where λ is the square of the ratio between the semi-axes of the elliptic cross-section of a vertical jet. The dashed trajectories divide the plane into two regions, all trajectories tending to $\lambda = 0$ in one and to $\lambda = \infty$ in the other.

above property. For example any trajectory which starts with $\dot{\lambda} = 0$ and $\lambda > 1{\cdot}07$ ultimately has $\lambda \to 0$. Thus the final flattening direction is generally that of the initial *minor* axis, when the initial jet is locally cylindrical. On the other hand, initially circular jets, with $\lambda = 1$, $|\dot{\lambda}| > 0{\cdot}2$, do tend to flatten in the direction which their initial *rate of change* of aspect ratio indicates. Those trajectories which asymptote to $\lambda = \infty$ do so along $\dot{\lambda} = +6\lambda$, i.e. have $\gamma \propto \xi^3$. The reciprocal property of (3.17) mentioned earlier is confirmed by figure 2; there is a correspondence between the behaviour near the origin and near infinity in this figure.

The zero-gravity situation studied by Taylor (1960) may be reconstructed by letting $g \to 0$ while keeping the original dimensional variable y in (1.6) fixed. This indicates that $t \to 0$ and hence (for $O(1)$ changes in λ) that $|\dot{\lambda}| \to \infty$ in (3.18). Thus (3.18) reduces to

$$\frac{d\dot{\lambda}}{d\lambda} = \frac{1}{4}\frac{5+3\lambda}{\lambda(1+\lambda)}\dot{\lambda}, \tag{3.19}$$

which integrates to give

$$\dot{\lambda} = A\lambda^{\frac{5}{4}}(1+\lambda)^{-\frac{1}{2}}. \tag{3.20}$$

The elliptic integral resulting from a further integration of (2.20) agrees with Taylor's (1960) equation (8). In figure 2, trajectories corresponding to the approximation (3.20) are the asymptotes as $\dot{\lambda} \to \pm\infty$.

4. Motion in parabolic arcs

We now suppose that the jet possesses an $O(1)$ horizontal component of velocity, and rises to a peak then falls. The origin of co-ordinates is chosen near the peak, at which point the dominant flow direction is horizontal and (after normalization) of unit magnitude to within an error $O(\epsilon^2)$.

It is 'intuitively clear' that such a free jet under gravity executes a parabolic arc of the same nature as a ballistic trajectory of a projectile. With the normalization chosen, this arc has equation

$$y = -\tfrac{1}{2}x^2. \tag{4.1}$$

Although a direct proof may be given (see, e.g., Keller & Geer 1973) that this is the correct zero-order limit as $\epsilon \to 0$, we shall instead assume this result, and merely show that an asymptotic expansion which begins in effect with (4.1) as the leading term is consistent.

It is convenient to work with a set of parabolic co-ordinates (ξ, η) defined by

$$x = \xi + \xi\eta, \quad y = -\tfrac{1}{2}\xi^2 + \eta + \tfrac{1}{2}\eta^2. \tag{4.2}$$

The change of co-ordinates from (x, y) to (ξ, η) is conformal, with

$$x + iy = (\xi + i\eta) - \tfrac{1}{2}i(\xi + i\eta)^2. \tag{4.3}$$

Hence the Laplace equation (1.1) transforms to

$$\phi_{\xi\xi} + \phi_{\eta\eta} + J\phi_{zz} = 0, \tag{4.4}$$

where the Jacobian J is given by

$$J = \partial(x, y)/\partial(\xi, \eta) = (1+\eta)^2 + \xi^2. \tag{4.5}$$

The top and bottom surfaces of the jet are assumed to be defined by

$$\eta = E_{\pm}(\xi, z), \tag{4.6}$$

where $E_+ \geqslant E_-$. The exact kinematic boundary condition on $\eta = E_{\pm}$ is

$$\phi_\eta = \phi_\xi E_{\pm\xi} + J\phi_z E_{\pm z}. \tag{4.7}$$

Similarly, the exact dynamic condition is obtained by setting $p = 0$ on $\eta = E_{\pm}$, where

$$-p = J^{-1}(\phi_\xi^2 + \phi_\eta^2) + \phi_z^2 - \xi^2 + 2\eta + \eta^2 - 1. \tag{4.8}$$

We now make the one-dimensional assumption that $E_\pm$ is a small quantity, $E_\pm = O(\epsilon)$, and that flow is mainly in the direction of increasing ξ, with magnitude $V(\xi)$ to be determined. The whole flow takes place in a region of small $\eta = O(\epsilon)$, where

$$x = \xi + O(\epsilon), \quad y = -\tfrac{1}{2}\xi^2 + O(\epsilon) = -\tfrac{1}{2}x^2 + O(\epsilon), \tag{4.9), (4.10}$$

and

$$J = 1 + \xi^2 + O(\epsilon). \tag{4.11}$$

Assuming

$$\phi = \phi_0(\xi) + \Phi(\xi, \eta, z), \tag{4.12}$$

where $\Phi = O(\epsilon^2)$ and $\partial/\partial\xi = O(1)$, whereas $\partial/\partial\eta$, $\partial/\partial z = O(\epsilon^{-1})$, we have from (4.4)

$$\Phi_{\eta\eta} + J\Phi_{zz} = -\phi_0''(\xi) + O(\epsilon^2), \tag{4.13}$$

which can be further approximated to

$$\Phi_{\eta\eta} + h^2\Phi_{zz} = -d(hV)/d\xi + O(\epsilon), \tag{4.14}$$

where

$$h(\xi) = (1+\xi^2)^{\frac{1}{2}} \tag{4.15}$$

and

$$V(\xi) = (1+\xi^2)^{-\frac{1}{2}}\phi_0'(\xi). \tag{4.16}$$

The corresponding approximation to the kinematic boundary condition (4.7) is

$$\Phi_\eta - h^2\Phi_z E_{\pm z} = hVE_{\pm\xi}, \tag{4.17}$$

while the dynamic condition (4.8) implies

$$(hV + \Phi_\xi)^2 + (\Phi_\eta)^2 + J\Phi_z^2 = J(1 + \xi^2 - 2\eta - \eta^2),$$

or, retaining only terms of order ϵ^2 or larger,

$$h^2V^2 + 2hV\Phi_\xi + \Phi_\eta + h^2\Phi_z^2 = (1+\xi^2)^2 - 4\eta^2. \tag{4.18}$$

The zero-order terms in (4.18) provide the velocity magnitude, i.e.

$$h^2V^2 = (1+\xi^2)^2,$$

or [from (4.10) and (4.15)]

$$V = (1-2y)^{\frac{1}{2}} + O(\epsilon). \tag{4.19}$$

This is the velocity of a projectile in the assumed normalized ballistic trajectory, confirming consistency of the zero-order assumption. The $O(\epsilon^2)$ terms in (4.18) require

$$-h^2p = 2h^2\Phi_\xi + \Phi_\eta^2 + h^2\Phi_z^2 + 4\eta^2 = 0 \tag{4.20}$$

on $\eta = E(\xi, z)$.

Our general task is to solve (4.14) subject to (4.17) and (4.20) on the unknown surface $\eta = E_\pm$. This task is even more difficult than that for the vertical jet, and again we shall restrict attention to elliptic-sectioned jets. Again, the case of two-dimensional waterfall-like sheets of water can be solved by the present method, giving results equivalent to those of previous investigators.

5. Parabolic jets with elliptic sections

We now attempt a solution

$$\Phi = A(\xi) + C(\xi)\eta^2 + D(\xi)z^2 \tag{5.1}$$

to (4.14), which is satisfied if

$$C + h^2D = -\xi. \tag{5.2}$$

The jet surface is taken to be defined by

$$\eta = \pm E_1(\xi, z), \tag{5.3}$$

where
$$E_1^2 = a^2(\xi) - \beta^2(\xi)\, z^2. \tag{5.4}$$

Thus the cross-section is assumed to be an ellipse in the η, z plane with centre at $\eta = 0$, with semi-axis $a(\xi)$ in the η direction (i.e. normal to the jet but in its plane) and with semi-axis $b = a/\beta$ in the z direction. The latter is a true length scale; however, the true half-height of the ellipse in the η direction is $h(\xi)\,a(\xi)$. It is again true that, without loss of generality, we can assume that Φ contains no terms in η, corresponding to choosing $\eta = 0$ as the centre-plane.

Now the kinematic boundary condition (4.17) implies that

$$\pm 2CE_1 - h^2(2Dz)\left(\frac{-\beta^2 z}{\pm E_1}\right) = h^2\left(\frac{aa' - \beta\beta' z^2}{\pm E_1}\right),$$

i.e.
$$(2Ca^2 - h^2 aa') + z^2(-2C\beta^2 + 2D\beta^2 h^2 + \beta\beta' h^2) = 0. \tag{5.5}$$

Thus
$$C = \tfrac{1}{2}h^2(a'/a), \tag{5.6}$$

and
$$C - Dh^2 = \tfrac{1}{2}h^2(\beta'/\beta). \tag{5.7}$$

Solving for C and D from (5.2) and (5.7) gives

$$4C = h^2(\beta'/\beta) - 2\xi, \tag{5.8}$$

and
$$-4h^2 D = h^2(\beta'/\beta) + 2\xi. \tag{5.9}$$

Equating the expressions for C in (5.6) and (5.8) leads to

$$a^2(1+\xi^2)/\beta = \text{constant},$$

or
$$Va^2 h/\beta = \text{constant},$$

or
$$V\pi(ah)\,b = \text{constant}, \tag{5.10}$$

which is the one-dimensional continuity equation again.

The dynamic boundary condition (4.20) gives in the present case

$$2h^2(A' + C'\eta^2 + D'z^2) + (2C\eta)^2 + h^2(2Dz)^2 + 4\eta^2 = 0. \tag{5.11}$$

On substitution of $\eta = \pm E_1$ we obtain

$$2h^2(A' + C'a^2) + 4a^2(1+C^2) + [2h^2(D' - C'\beta^2) - 4C^2\beta^2 + 4D^2h^2 - 4\beta^2]\,z^2 = 0. \tag{5.12}$$

Thus
$$A' = -a^2C' - 2a^2(1+C^2)/h^2 \tag{5.13}$$

and
$$h^2(D' + 2D^2 - \beta^2 C') = 2\beta^2(1+C^2). \tag{5.14}$$

Equation (5.14) does not involve A' and can be used to solve for the eccentricity of the ellipse as follows. We first use (5.2) to eliminate C, obtaining

$$D'(1 + h^2\beta^2) + 2D^2(1 - h^2\beta^2) = \beta^2(1 + 2\xi D). \tag{5.15}$$

It is appropriate at this point to introduce the true aspect ratio

$$\gamma = h\beta \tag{5.16}$$

of the ellipse in physical co-ordinates, giving finally

$$D'(1+\gamma^2)+2D^2(1-\gamma^2)=\frac{\gamma^2}{1+\xi^2}(1+2\xi D) \tag{5.17}$$

together with (5.9), i.e. $$\gamma' = -\gamma[4D+\xi/(1+\xi^2)]. \tag{5.18}$$

Equations (5.17) and (5.18) reduce to (3.13) and (3.14) respectively as $\xi\to\infty$. This is to be expected, since in that limit we lose the effect of the curvature of the jet, and are involved again with a vertically falling jet. The co-ordinate ξ asymptotes to $(-2y)^{\frac{1}{2}}$ as $\xi\to\infty$, both here and in §3. The quantity D can if required be eliminated from (5.17) and (5.18) to give a nonlinear second-order ordinary differential equation for γ, analogous to (3.17).

On the other hand, in the present case no change of variables such as (3.16) can be used to make the system autonomous, and no unique phase-plane plots such as figure 2 can be presented. We have chosen to solve (5.17) and (5.18) numerically as they stand, and present in figures 3–5 some examples of computed results for $\gamma(\xi)$ for various assumed starting configurations.

It should first be noted that, if we commence an integration of (5.17) and (5.18) at a value $\xi = \xi_0$, then the angle the jet makes with the horizontal at that point is α, where

$$\tan\alpha = -\xi_0. \tag{5.19}$$

Although the present paper concerns solely *free* jets, we have in mind eventual application to jets from nozzles, which would require matching of the present flow to an exit flow from a rigid pipe. It is therefore appropriate to discuss our solution from the point of view of the (probable) parameters of the nozzle, one of which is its angle of inclination α given by (5.19).

Circular initial cross-sections (i.e. $\gamma = 1$) are clearly of particular interest, as are cross-sections which are initially locally stationary in eccentricity, with $d\gamma/d\xi = 0$. In figure 3 we show the variation with ξ of the aspect ratio γ for such initial conditions, for various choices of the initial value ξ_0, or equivalently of the inclination α. The aspect ratio decreases monotonically to zero along the jet in all cases. It is also clear that the jet thickens substantially in side view at the top of the arc, i.e. that the semi-axis ha in the η direction increases. The semi-axis b in the (horizontal) z direction changes much less, but does appear to decrease somewhat. For example the thickness in top view at the top of the arc is less than the initial diameter for initial inclinations less than about 65°. The above features of the flow appear to be in at least qualitative agreement with observation.

One may wish to design nozzles which maintain a circular cross-section over the top of the arc. Since a circular initial cross-section ($\gamma = 1$) deforms in such a way that it develops a major axis in a vertical plane (i.e. $\gamma < 1$), it is plausible that one way to achieve this is to start with an elliptical cross-section with its major axis horizontal, i.e. with $\gamma > 1$. However, so long as $d\gamma/d\xi = 0$ initially, this is generally fruitless, since the rate of change of eccentricity increases rapidly with initial eccentricity. The major axis tends to become vertical at the top of the arc, and in every case becomes vertical far downstream. This is illustrated by figure 4, which shows the value of γ at $\xi = 0$, plotted against the

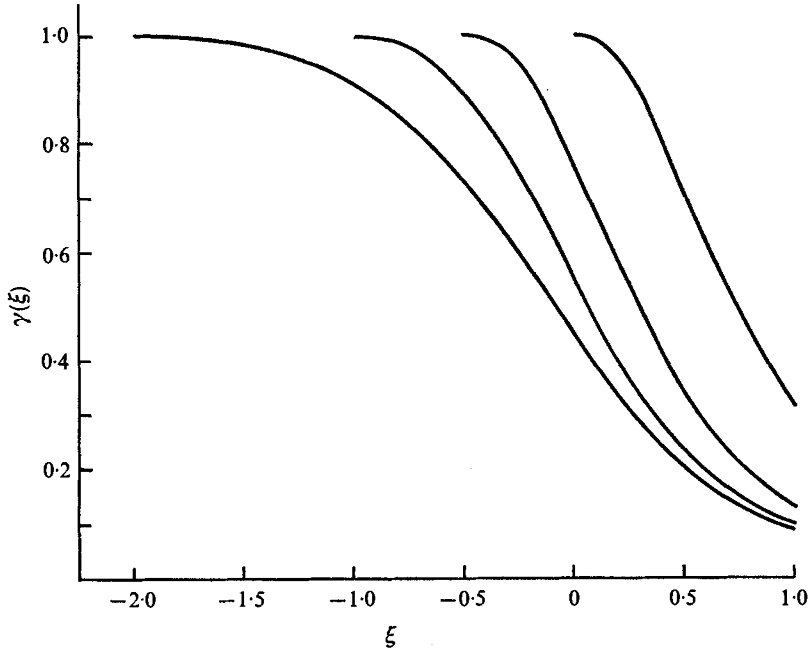

FIGURE 3. Variation along the jet of the aspect ratio of an elliptical-sectioned parabolic-arc jet, whose initial cross-section is circular and locally stationary in eccentricity. The initial value of ξ on each curve defines the initial angle of the jet, as in (5.19).

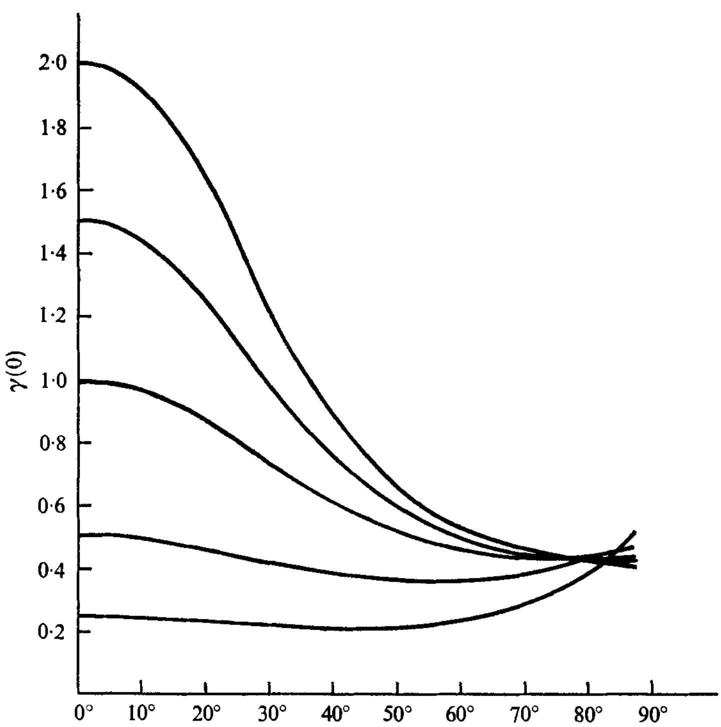

FIGURE 4. Effect of initial aspect ratio. Top-of-arc value of aspect ratio, for an elliptic-sectioned parabolic-arc jet, as a function of initial angle, for various starting aspect ratios and a zero initial rate of change of aspect ratio.

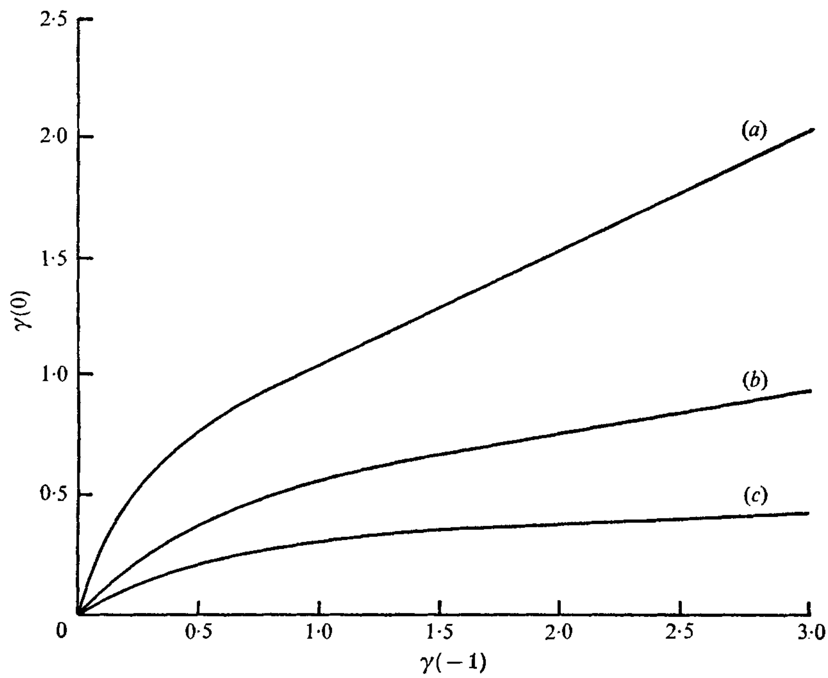

FIGURE 5. Effect of initial rate of change of aspect ratio. Top-of-arc value of aspect ratio, for an elliptic-sectioned parabolic-arc jet, as a function of initial aspect ratio, for an initial angle of 45°, and three initial values of the ratio γ'/γ. (*a*) $\gamma'(-1) = \gamma(-1)$, (*b*) $\gamma'(-1) = 0$, (*c*) $\gamma'(-1) = -\gamma(-1)$.

initial inclination α. Each separate curve corresponds to a different initial value of γ, indicated by the value of $\gamma(0)$ at $\alpha = 0$. For example, if $\alpha = 45°$, the major axis at the top of the arc is vertical unless the initial aspect ratio exceeds about 3·25. These results could have been inferred from figure 2, which indicated that, when $d\gamma/d\xi$ is initially zero, there is a tendency for the final flattening direction to be perpendicular to that initially.

Finally, in figure 5 we indicate the effect of the initial *rate of change* of eccentricity. In this figure we plot the computed aspect ratio $\gamma(0)$ at the top of the arc against the initial aspect ratio $\gamma(0)$ for $\xi_0 = -1$, i.e. for a 45° initial angle of inclination, and for $\gamma'(-1)/\gamma(-1) = 0, \pm 1$. There is again a strong tendency for γ to decrease, even when $\gamma' > 0$ initially, and the final theoretical state is always $\gamma = 0$, i.e. flattening in the plane of the arc. Of course in practice the jet breaks up soon after the top of the arc. The question of the appropriate theoretical direction and extent of flattening well beyond the top of the arc is relevant to the rapidity of this breakup.

6. Conclusion

The problem of determination of the shape of the cross-section of a free jet has been reduced to that of solving a sequence of two-dimensional boundary-value problems in the cross-flow plane. These are free-surface problems with an unknown boundary, on which both kinematic and dynamic boundary conditions must hold. In its most general form this problem is probably intractable; however, some further effort may be worth while on it, e.g. for some simple initial cross-sections such as the triangular shape for which Bidone's striking observations were described by Rayleigh (1945, p. 356).

In the present paper we have contented ourselves with a study of elliptical cross-sections, which are capable of staying elliptical as they propagate. The task is then to compute the parameters of the ellipse as functions of distance along the arc. We have shown how the aspect ratio or the eccentricity of the ellipse can be found by solving a nonlinear second-order ordinary differential equation. The solution depends on the choice of the initial conditions for the eccentricity and its rate of change. Once this equation is solved, we can then if required use (3.10) or (5.13) to determine the $O(\epsilon^2)$ correction to the main flow along that trajectory and hence the pressure distribution across the jet, which is parabolic, with a positive maximum at the centre of the jet. Since the one-dimensional continuity equation (2.5) determines the cross-sectional area of the ellipse, a knowledge of its eccentricity also enables the separate major and minor axes to be established.

It has been tacitly assumed here that the free jets considered can be matched to exit flows from orifices. If for example the orifice is a straight pipe, the values of the eccentricity and its rate of change are those appropriate to the pipe ending. Although this is likely to be true for such straight pipes, the choice of the appropriate initial conditions when the jet emerges from holes, spillways etc. is not at all clear. A survey of procedures for carrying out such matching for flows through small holes in two or three dimensions is given by Tuck (1975*a*).

The present work and most (but see Conway 1967; Keady & Norbury 1975) of that by previous authors has concerned *thin* jets. It is of interest to consider the behaviour as the thickness increases. The effective thickness ϵ defined by (1.9) can become large either if the flow rate δ is large or if the velocity scale U is small. In the case of a parabolic arc, U is the *horizontal* velocity, so that (at fixed exit velocity magnitude) we can make ϵ large by making the jet's initial inclination more nearly vertical. The ultimate effect is of course that the jet falls back on itself, and the assumed single-branched nearly parabolic arc is no longer a valid topology for the flow. Some of the existence and uniqueness questions which arise in this and related free-surface problems (cf. Tuck 1975*b*) are of practical interest.

I wish to acknowledge the usefulness of critical discussion of this work with Dr L. Schwartz.

REFERENCES

Chandrasekhar, S. 1968 *Hydrodynamic and Hydromagnetic Stability*. Oxford: Clarendon Press.

Clarke, N. S. 1965 On two-dimensional inviscid flow in a waterfall. *J. Fluid Mech.* **22**, 359–369.

Conway, W. E. 1967 The two-dimensional vertical jet under gravity. *J. Math. Anal. Appl.* **19**, 282–290.

Friedrichs, K. O. 1948 Derivation of the shallow water theory. *Comm. Pure Appl. Math.* **1**, 81–88.

Keady, G. 1973 The jet from a horizontal slot at large Froude number. *Proc. Camb. Phil. Soc.* **73**, 515–529.

Keady, G. & Norbury, J. 1975 The jet from a horizontal slot under gravity. *Proc. Roy. Soc.* A **344**, 471–487.

Keller, J. B. & Geer, J. 1973 Flows of thin streams with free boundaries. *J. Fluid Mech.* **59**, 417–432.

Keller, J. B., Rubinow, S. I. & Tu, Y. O. 1973 Spatial instability of a jet. *Phys. Fluids*, **16**, 2052–2055.

Keller, J. B. & Wietz, M. L. 1957 A theory of thin jets. *9th Int. Cong. Appl. Mech. (Brussels)*, pp. 316–323.

Lamb, H. 1932 *Hydrodynamics*, 5th edn. Cambridge University Press.

Longuet-Higgins, M. S. 1972 A class of exact, time-dependent, free-surface flows. *J. Fluid Mech.* **55**, 529–543.

Rayleigh, Lord 1945 *The Theory of Sound*, vol. 2, 2nd edn republication. Dover.

Shapiro, A. 1953 *The Dynamics and Thermodynamics of Compressible Fluid Flow*, vol. 1. New York: Ronald.

Streeter, V. L. (ed.) 1961 *Handbook of Fluid Dynamics*. McGraw-Hill.

Taylor, G. I. 1960 Formation of thin flat sheets of water. *Proc. Roy. Soc.* A **259**, 1–17.

Tuck, E. O. 1974 One-dimensional flows as slender-body problems, with applications to ships moving in channels. *Proc. Workshop on Slender-Body Theory, Ann Arbor, June* 1973. *Univ. Michigan Rep. N.A.M.E.* no. 164, pp. 27–35.

Tuck, E. O. 1975*a* Matching problems involving flow through small holes. *Adv. Appl. Mech.* **15**, 89–158.

Tuck, E. O. 1975*b* On air flow over free surfaces of stationary water. *J. Austr. Math. Soc.* B **19**, 66–80.